35th Annual International Conference of the IEEE EMBS
Osaka, Japan, 3 - 7 July, 2013

Three-dimensional modeling of oxidized-LDL accumulation and HDL mass transport in a coronary artery: A proof-of-concept study for predicting the region of atherosclerotic plaque development

Antonis I. Sakellarios, Panagiotis K. Siogkas, Lambros S. Athanasiou, Themis P. Exarchos, *Member, IEEE*, Michail I. Papafaklis, Christos V. Bourantas, Katerina K. Naka, Lampros K. Michalis, Nenad Filipovic, Oberdan Parodi and Dimitrios I. Fotiadis, *Senior Member, IEEE*

Abstract— **Low density lipoprotein (LDL) has a significant role on the atherosclerotic plaque development, while the concentration of high density lipoproteins (HDL) is considered to play an atheroprotective role according to several biochemical mechanisms. In this work, it is the first time that both LDL and HDL concentrations are taken into account in order to predict the regions prone for plaque development. Our modeling approach is based on the use of a realistic three-dimensional reconstructed pig coronary artery in two time points. Biochemical data measured in the pig were also included in order to develop a more customized model. We modeled coronary blood flow by solving the Navier-Stokes equations in the arterial lumen and plasma filtration in the arterial wall using Darcy's Law. HDL transport was modeled only in the arterial lumen using the convection-diffusion equation, while LDL transport was modeled both in the lumen and the arterial wall. An additional novelty of this work is that we model the oxidation of LDL taking into account the atheroprotective role of HDL. The results of our model were in good agreement with histological findings demonstrating that increased oxidized LDL is found near regions of advanced plaques, while non-oxidized LDL is found in regions of early plaque types.**

I. Introduction

Coronary artery disease (CAD) is the most common cause of death in western societies [1]. Atherosclerosis is characterized by the thickening of the arterial wall which may lead to occlusion of the arterial lumen. There are many risk factors reponsible for atherosclerotic plaque development including hyperlipidemia, hypertension, diabetes, smoking, genetic disorders. An increased concentration of LDL is found to have an utmost role at the initial stages of plaque formation since the augmented accumulation of lipids in the arterial wall is related to the inflammatory process. LDL particles accumulating in the arterial wall are gradually being oxidized (ox-LDL) and subsequently, foam cells are formed by the phagocytosis of the ox-LDL by macrophages. In contrast, HDL has an atheroprotective role since it is considered to protect from LDL oxidation [2] and also limits the inflammatory process that underlies plaque initiation [3]. The anti-oxidative role of HDL is in part due to the paraoxonase enzyme contained in the HDL particle [3] and prevents oxidation by hydrolyzing cholesterol and lipid peroxides [4].

Several modeling approaches have been proposed for understanding the mechanisms of plaque initiation. The majority of these studies are based on the modeling of LDL transport in arterial segments. The main classification of these approaches can be made according to the boundary conditions that are applied at the lumen-endothelium interface. Some studies consider a non-permeable endothelium, where LDL is calculated in the luminal area only [5]. However, more recent studies treat the endothelium as a semi-permeable membrane and several conditions are important in order to represent the physiology of the artery. The Kedem-Katchalksy equations [6] are widely used to describe endothelial permeability [7-9]. In other studies the role of mitosis is taken into account and its influence on the total accumulated LDL concentration [10, 11]. Finally, in latest computational studies [12, 13] the overall process of plaque formation is modeled assuming LDL transport, monocyte and LDL-oxidation modeling, foam cell formation and plaque formation.

In the present study, we model both LDL and HDL transport in a reconstructed arterial segment. We consider that the endothelial layer is permeable and we use the Kedem-Katchalsky equations to describe the penetration of the molecules in the wall. The novelty of this work is two-fold: 1) we model HDL transport, and 2) we model LDL oxidation taking into account the protective role of the accumulating HDL in the wall. Moreover, this computational study is considered as a proof-of-concept study for predicting the localization of lipid-rich regions, which are expected to culminate in advanced plaques associated with clinical events. For this purpose, we use the three-

This work was supported by the EU project ARTreat FP7-224297, Multi-level patient-specific artery and atherogenesis model for outcome prediction, decision support treatment, and virtual hand-on training.

A.I. Sakellarios, L.S. Athanasiou, P.K. Siogkas and D.I. Fotiadis are with the Unit of Medical Technology and Intelligent Information Systems, Dept. of Materials Science and Engineering, University of Ioannina, GR 45110 (email: ansakel@cc.uoi.gr, lmathanas@cc.uoi.gr, psiogkas@cc.uoi.gr corresponding author phone: +302651008803; fax: +302651008889; e-mail: fotiadis@cs.uoi.gr).

T.P. Exarchos is with the Institute of Molecular Biology and Biotechnology, Dept. of Biomedical Research, FORTH, GR45110, Ioannina, Greece (email: exarchos@cc.uoi.gr)

M.I Papafaklis is with the Cardiovascular Division, Brigham and Women's Hospital, Harvard Medical School, Boston, USA (email: m.papafaklis@yahoo.com)

C.V. Bourantas is with the Dept. of Interventional Cardiology, Erasmus MC, Thoraxcenter, Rotterdam, The Netherlands (email: cbourantas@gmail.com)

K.K. Naka and L.K. Michalis are with the Michaelideion Cardiac Center, Dept. of Cardiology in Medical School, University of Ioannina, GR 45110 Ioannina, Greece (email: anaka@cc.uoi.gr, lmihalis@cc.uoi.gr).

N. Filipovic is with the University of Kragujevac, Serbia (e-mail: fica@kg.ac.rs)

O. Parodi is with the Institute of Clinical Physiology, National Research Council, 56124, Pisa, Italy (email: oberpar@tin.it)

dimensional reconstruction of a pig coronary artery at two time points (baseline, follow-up) for our modeling analyses and we correlate our results with histolopathologic findings at follow-up after sacrifice taking into account biochemical, biological and genetic markers.

II. Material and Methods

A. Proof-of-Concept Data

In this study, we use data from a pig that received a high-lipid diet for 16 weeks; the animal underwent coronary angiography, Doppler flow velocimetry, and IVUS evaluation at baseline and at the end of the diet period before sacrifice (Fig. 1). Ex vivo micro-CT analysis of excised coronary left main and left anterior descending arteries was performed to accurately assess the severity of lesions (Fig. 2A), which were also analyzed by histology and immunohistochemistry (Fig. 2B).

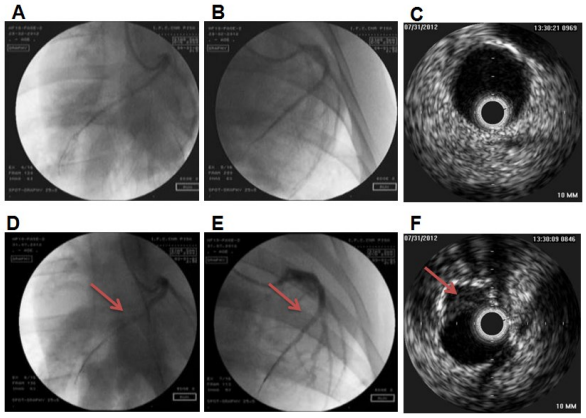

Figure 1: X-ray coronary angiography images at 0 weeks from two different views (A and B), and after 16 weeks of diet (D and E). Intravascular ultrasound images (IVUS) of the left anterior descending artery: (C) normal vessel, (F) vessel with lesion. Red arrows show the angiographic location of a lesion as seen in the IVUS image (F).

Blood samples were collected at baseline and follow-up catheterization. The plasma lipid profile, i.e. total cholesterol, HDL-cholesterol (HDL-C) and LDL-cholesterol (LDL-C) was measured.

Three-dimensional coronary artery reconstruction was performed using the IVUS and angiographic data using a well validated algorithm [14].

B. Modeling of Fluid Dynamics

Blood flow in the arterial lumen was modeled using the Navier-Stokes equations and the continuity equation:

$$-\mu\nabla^2\mathbf{u}_l + \rho(\mathbf{u}_l\cdot\nabla)\mathbf{u}_l + \nabla p_l = 0\,, \qquad (1)$$

$$\nabla\cdot\mathbf{u}_l = 0\,, \qquad (2)$$

where l refers to the lumen, $\mathbf{u}_l$ is the blood velocity, p_l is the pressure, μ is the dynamic viscosity of blood, and ρ is the blood density.

Plasma filtration in the arterial wall was modeled using Darcy's Law:

$$u_w - \nabla\cdot\left(\frac{\kappa_w}{\mu_p}p_w\right) = 0\,, \qquad (3)$$

where p_w is the pressure in the arterial wall and u_w is the plasma velocity and k_w is the Darcian permeability.

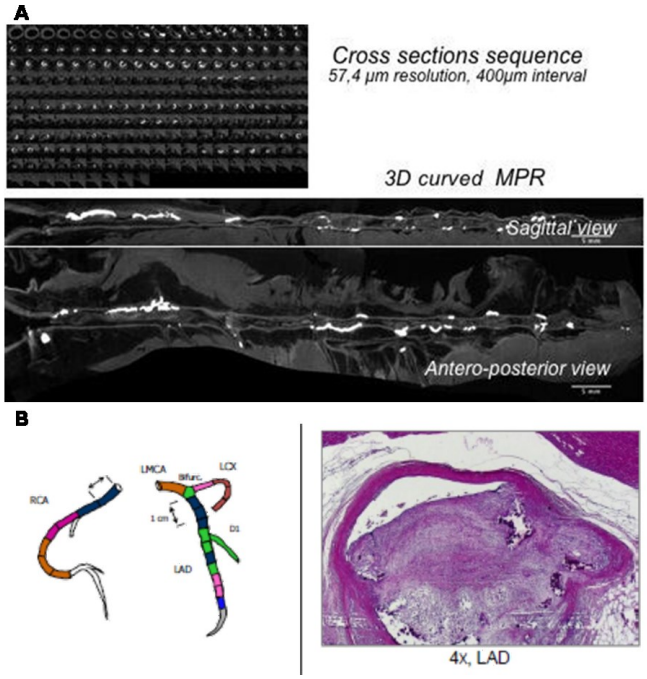

Figure 2: Imaging processing of micro-CT analysis of the left main coronary artery and left anterior descending artery (LAD). All acquired frames at 57.4 µm^3 voxel resolution (A) were processed by Osirix and MPR longitudinal 3D reconstruction. (B-left) Colors represent the lesion type. (B-right) A typical histological frame of the LAD.

An artery-specific flow was applied at the inlet of the artery using the Doppler flow velocimetry measurements. At the endothelial boundary we applied a transmural velocity normal to the boundary layer. All parameters used in the study are summarized in Table 1.

C. Modeling of Mass transport

We modeled LDL and HDL transport in the arterial lumen using the convection-diffusion equations:

$$\nabla\cdot\left(-D_{l,LDL}\nabla c_{l,LDL} + c_l u_{l,LDL}\right) = 0\,, \qquad (4)$$

$$\nabla\cdot\left(-D_{l,HDL}\nabla c_{l,HDL} + c_l u_{l,HDL}\right) = 0\,, \qquad (5)$$

where l indicates the lumen domain, *LDL* and *HDL* the molecules which are transported, D is the diffusivity in the lumen and c is the molecule concentration.

In parallel, we modeled LDL transport in the arterial wall and also the oxidation of LDL depending on the luminal HDL concentration. LDL transport in the wall was modeled using the convection-diffusion-reaction equation:

$$\nabla\cdot\left(-D_{w,LDL}\nabla c_{w,LDL} + kc_{w,LDL}u_{w,LDL}\right) = r_{w,LDL}c_{w,LDL}\,, \qquad (6)$$

where D_w is the diffusivity in the wall, k is the solute lag coefficient and r_w is the consumption rate constant.

The boundary conditions applied for mass transport were a constant concentration for LDL ($C_{0,LDL}$) and HDL ($C_{0,HDL}$) at the inlet (using the measured serum values) and the adventitia boundary ($0.005C_0$), a convective flow at the outlet of the artery, and a coupling system of equations at both sides of the endothelial boundary. The coupling system, which defines the interaction between the lumen and the arterial wall was described by the Kedem-Katchalsky equations:

$$J_v = L_p\left(\Delta p - \sigma_d \Delta \pi\right), \quad (7)$$

$$J_s = P\Delta c + \left(1-\sigma_f\right)J_v \bar{c}, \quad (8)$$

where L_p is the hydraulic conductivity of the endothelium; Δc is the solute concentration difference, Δp is the pressure drop and $\Delta \pi$ is the oncotic pressure difference, in the endothelium; σ_d is the osmotic reflection coefficient, σ_f is the solvent reflection coefficient, P is the solute endothelial permeability, and $\bar{c}$ is the mean endothelial concentration. The oncotic pressure difference $\Delta \pi$ was neglected in our simulations because of the decoupling of the fluid dynamics from the solute dynamics. We assumed that hydraulic conductivity was dependent on wall shear stress (WSS) in accordance with the studies presented by Sun et al. [7, 9].

D. Modeling of LDL oxidation

LDL oxidation was modeled taking into account the atheroprotective role of HDL which necessitates the quantification of the HDL protective role. Data presented in [15] were used for this purpose. Thus, the data presented in the previous *in vitro* experimental study were fitted to an HDL-C concentration of 40 mg/dl, which represents *in vivo* conditions in humans. Furthermore, in order to translate the LDL-C and HDL-C concentrations into LDL and HDL particle concentrations which are the ones considered actually for mass transport, we used the following conversions based on human data: (a) 100 mg/dl LDL-C equals to approximately 1060 nmol/lt of LDL particles [16], and (b) 60 mg/dl HDL-C equals to approximately 36 μmol/lt [17]. Due to the lack of experimental data, in this preliminary study, we assumed that the transport properties of HDL are similar to those of LDL.

The oxidation of LDL was modeled using a diffusion-reaction equation:

$$d\Delta O + O \cdot M + r_{w,LDL} c_{w,LDL} + HDL_{protection} = 0, \quad (9)$$

where O is the oxidized LDL, d is the diffusion coefficient and M is the number of white blood cells. The equation requires as inlet boundary condition the calculated LDL concentration, while the reaction term of the equation takes into account the HDL concentration. $HDL_{protection}$ was defined by the experimentally observed relation shown in Fig. 3.

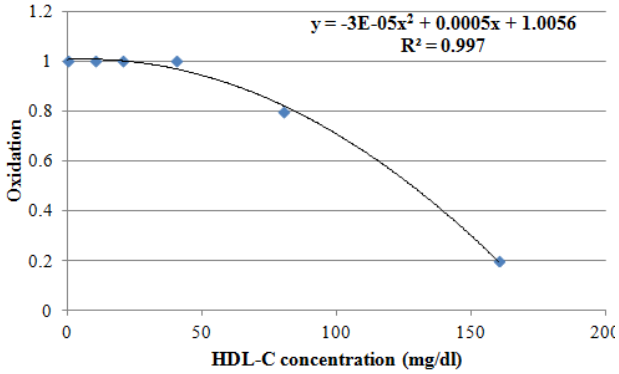

Figure 3: Relation of LDL oxidation with HDL-cholesterol concentration. Data initially presented in [15] are fitted to represent realistic values.

III. Results - Discussion

According to the analysis of histological images and micro-CT data, it was found that the average lesion area was 1.93 mm^2 with a max lesion area of 6.56 mm^2. At the region of max lesion area (Fig. 4, red arrow), the max intima thickness (2700 μm) was found and there was a large fibrolipid core (45% of total wall area). However, the maximum proportion of lipid accumulation was found in a more distal region (22% of total wall area) (Fig. 4, blue arrow).

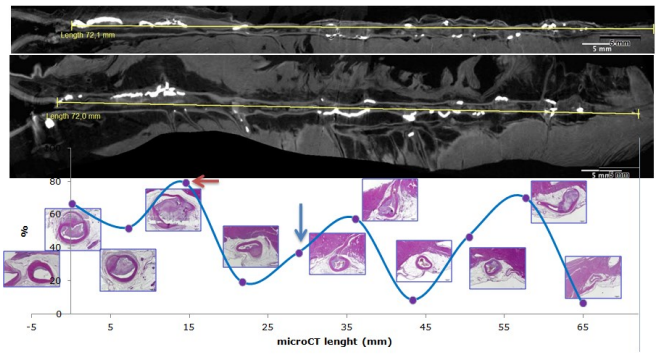

Figure 4: Micro-CT assisted histomorphometric profiling of the left anterior descending coronary artery. The red arrow depicts the region of max lesion area and the blue arrow shows the region of max lipid accumulation.

The results of the computational study showed an average WSS value of 1.5 Pa and average normalized wall LDL concentration of 0.11. The distribution of the values is shown in Fig. 5. It is clear that LDL accumulation depends on the local distribution of WSS. This is caused by the concentration polarization from the luminal side of the endothelium.

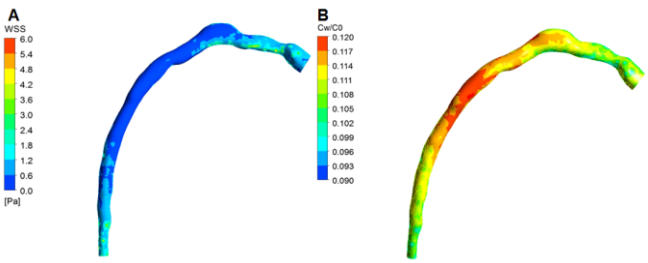

Figure 5: (A) WSS distribution. (B) Normalized LDL concentration. LDL accumulation is increased at the region of low WSS.

Table I. PARAMETER VALUES USED IN THE SIMULATION.

Parameter	Value	Parameter	Value
Blood density (ρ)	1060 Kg/m^3	Pressure (p)	70 mmHg
Lumen diffusivity (D_l)	5×10^{-12} m^2/s	Solute lag coefficient (K_{lag})	0.1486
Endothelial permeability (P)	1.5×10^{-10} m/s	Initial LDL concentration ($C_{0,LDL}$)	48.4 mg/dl
Wall diffusivity (D_w)	8×10^{-13} m^2/s	Initial HDL concentration ($C_{0,HDL}$)	32 mg/dl
Solvent reflection coefficient (σ_d)	0.997	LDL degradation rate (r_w)	1.4×10^{-4}
Blood viscosity (μ)	0.0035 Pa·s	Pressure in the arterial wall (p_w)	17.5 mmHg
Darcian permeability (k_w)	1.2×10^{-18} m^2	Plasma viscosity (μ_p)	0.001 Pa·s

Figure 6 depicts the distribution of oxidized LDL. Comparing the results of LDL concentration with the oxidized LDL, we conclude that LDL accumulation is more broadly dispersed in the wall compared to oxidized LDL. LDL accumulated at the middle part of the arterial segment corresponding to the region of max lipidic proportion in histopathology, while oxidized LDL had an increased value at a small region corresponding to the largest lesion in histology. The co-localization of the focally increased computed oxidized LDL accumulation with the largest lesion is in agreement with the augmented inflammatory/oxidative processes observed in advanced atherosclerotic lesions.

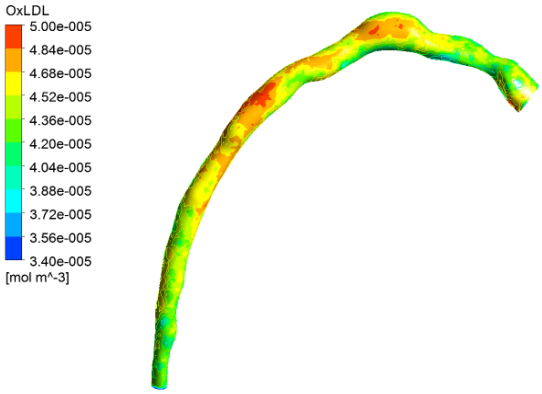

Figure 6: Distribution of oxidized LDL.

IV. CONCLUSION

In the current work, we present a novel model computing the oxidized LDL accumulation in the arterial wall. Our approach takes into account both LDL and HDL transport in arteries accounting for the atheroprotective effect of HDL as an antioxidant factor for LDL. The model was applied to a realistic geometry of a pig coronary artery using measured biochemical data and a direct comparison was made with histology. The main limitation of this approach is the lack of experimental data about the transport properties of HDL. The current study demonstrates that complex computational models representing more realistically the patho-physiological processes of atherosclerosis may provide an increased predictive value for identifying regions at highest risk for development of advanced lesions.

REFERENCES

[1] World Health Organization. Cardiovascular Diseases, 2009.

[2] A. Kontush and M. J. Chapman, "Antiatherogenic function of HDL particle subpopulations: focus on antioxidative activities," Current Opinion in Lipidology, vol. 21, pp. 312-318, Aug 2010.

[3] P. Barter, "The role of HDL-cholesterol in preventing atherosclerotic disease," European Heart Journal Supplements, vol. 7, pp. F4-F8, Jul 2005.

[4] A. Mertens and P. Holvoet, "Oxidized LDL and HDL: antagonists in atherothrombosis," Faseb Journal, vol. 15, pp. 2073-2084, Oct 2001.

[5] M. Prosi, P. Zunino, K. Perktold, and A. Quarteroni, "Mathematical and numerical models for transfer of low-density lipoproteins through the arterial walls: a new methodology for the model set up with applications to the study of disturbed lumenal flow," J Biomech, vol. 38, pp. 903-17, Apr 2005.

[6] O. Kedem and A. Katchalsky, "Thermodynamic analysis of the permeability of biological membranes to non-electrolytes," Biochim Biophys Acta, vol. 27, pp. 229-46, Feb 1958.

[7] N. Sun, R. Torii, N. B. Wood, A. D. Hughes, S. A. Thom, and X. Y. Xu, "Computational modeling of LDL and albumin transport in an in vivo CT image-based human right coronary artery," J Biomech Eng, vol. 131, p. 021003, Feb 2009.

[8] N. Sun, N. B. Wood, A. D. Hughes, S. A. Thom, and X. Y. Xu, "Influence of pulsatile flow on LDL transport in the arterial wall," Ann Biomed Eng, vol. 35, pp. 1782-90, Oct 2007.

[9] N. Sun, N. B. Wood, A. D. Hughes, S. A. Thom, and X. Y. Xu, "Fluid-wall modelling of mass transfer in an axisymmetric stenosis: effects of shear-dependent transport properties," Ann Biomed Eng, vol. 34, pp. 1119-28, Jul 2006.

[10] U. Olgac, V. Kurtcuoglu, and D. Poulikakos, "Computational modeling of coupled blood-wall mass transport of LDL: effects of local wall shear stress," American Journal of Physiology-Heart and Circulatory Physiology, vol. 294, pp. H909-H919, Feb 2008.

[11] U. Olgac, D. Poulikakos, S. C. Saur, H. Alkadhi, and V. Kurtcuoglu, "Patient-specific three-dimensional simulation of LDL accumulation in a human left coronary artery in its healthy and atherosclerotic states," American Journal of Physiology-Heart and Circulatory Physiology, vol. 296, pp. H1969-H1982, Jun 2009.

[12] N. Filipovic, et al., "ARTreat Project: Three-Dimensional Numerical Simulation of Plaque Formation and Development in the Arteries," Ieee Transactions on Information Technology in Biomedicine, vol. 16, pp. 272-278, Mar 2012.

[13] O. Parodi, et al., "Patient-Specific Prediction of Coronary Plaque Growth From CTA Angiography: A Multiscale Model for Plaque Formation and Progression," Ieee Transactions on Information Technology in Biomedicine, vol. 16, pp. 952-965, Sep 2012.

[14] C. V. Bourantas, I. C. Kourtis, M. E. Plissiti, D. I. Fotiadis, C. S. Katsouras, M. I. Papafaklis, and L. K. Michalis, "A method for 3D reconstruction of coronary arteries using biplane angiography and intravascular ultrasound images," Computerized Medical Imaging and Graphics, vol. 29, pp. 597-606, Dec 2005.

[15] S. T. Kunitake, M. R. Jarvis, R. L. Hamilton, and J. P. Kane, "Binding of Transition-Metals by Apolipoprotein-a-I-Containing Plasma-Lipoproteins - Inhibition of Oxidation of Low-Density Lipoproteins," Proceedings of the National Academy of Sciences of the United States of America, vol. 89, pp. 6993-6997, Aug 1 1992.

[16] J. D. Otvos, S. Mora, I. Shalaurova, P. Greenland, R. H. Mackey, and D. C. Goff, "Clinical implications of discordance between low-density lipoprotein cholesterol and particle number," Journal of Clinical Lipidology, vol. 5, pp. 105-113, Apr 2011.

[17] R. H. Mackey, P. Greenland, D. C. Goff, D. Lloyd-Jones, C. T. Sibley, and S. Mora, "High-Density Lipoprotein Cholesterol and Particle Concentrations, Carotid Atherosclerosis, and Coronary Events MESA (Multi-Ethnic Study of Atherosclerosis)," Journal of the American College of Cardiology, vol. 60, pp. 508-516, Aug 7 2012.